

# Redesign of Cosubstrate Specificity and Identification of Important Residues for Substrate Binding to hChAT<sup>†</sup>

Keith D. Green,<sup>§</sup> Vanessa R. Porter,<sup>‡,§</sup> Yaru Zhang,<sup>§,||</sup> and Sylvie Garneau-Tsodikova<sup>\*,‡,§,||</sup>

<sup>‡</sup>Department of Medicinal Chemistry, <sup>§</sup>Life Sciences Institute, 210 Washtenaw Avenue, and <sup>||</sup>Chemical Biology Doctoral Program, University of Michigan, Ann Arbor, Michigan 48109-2216

Received May 19, 2010; Revised Manuscript Received June 15, 2010

**ABSTRACT:** In eukaryotes, choline acetyltransferase (ChAT) catalyzes the reversible formation of the neurotransmitter acetylcholine from choline and acetyl-CoA. ChAT belongs to a family of CoA-dependent enzymes that also includes the carnitine acyltransferases CrAT, CrOT, and CPTs. In contrast to CrOT and CPTs that are very active toward medium- and long-chain acyl-CoAs, respectively, CrAT and ChAT display activity toward only short-chain acyl-CoAs. We recently demonstrated the substrate and cosubstrate promiscuity of the wild-type human ChAT (hChAT). To extend the flexibility of this enzyme, we have generated a series of single, double, and triple hChAT mutants. Here we report the conversion of hChAT into choline octanoyltransferase (ChOT) and choline palmitoyltransferase (ChPT). The E337 and C550 residues (numbering from hChAT) were previously shown to dictate the acyl-CoA cosubstrate specificity in the carnitine series. Here we identify and demonstrate the importance of C551, in addition to E337 and C550, in contributing to the acyl-CoA specificity of hChAT. We also show that either C550 or C551 needs to be present for the transfer of medium- and long-chain acyl-CoAs by hChAT. By exploring the potential expansion of the tunnel on the substrate side, we demonstrate that residues M84, Y436, and Y552 play a critical role in binding and holding the choline substrate in the ChAT active site.

Choline acetyltransferase (ChAT)<sup>1</sup> catalyzes the reversible transfer of the acetyl moiety of acetyl-CoA to choline for the formation of the neurotransmitter acetylcholine (ACh) (Figure 1A). ACh is widely distributed in the central and peripheral nervous systems as well as in non-nervous tissues and thus plays an important role in a variety of brain and basic cellular functions. A number of syndromes and neurodegenerative disorders, including Alzheimer's disease (AD) (1), amyotrophic lateral sclerosis (2), schizophrenia (3), Huntington's disease (HD) (4), sudden infant death syndrome (5), and Rett syndrome (6), have been correlated with diminished ACh levels associated with decreased ChAT activity.

ChAT belongs to a family of CoA-dependent acyltransferases that also includes dihydrolipoyl transacetylase, chloramphenicol acetyltransferase (CAT), carnitine acetyltransferase (CrAT), carnitine octanoyltransferase (CrOT), and carnitine palmitoyltransferases (CPTI and CPTII) (7). The carnitine acyltransferases are enzymes involved in the  $\beta$ -oxidation of fatty acids that catalyze a reaction similar to that catalyzed by ChAT but utilize carnitine instead of choline as their substrate and differ in the

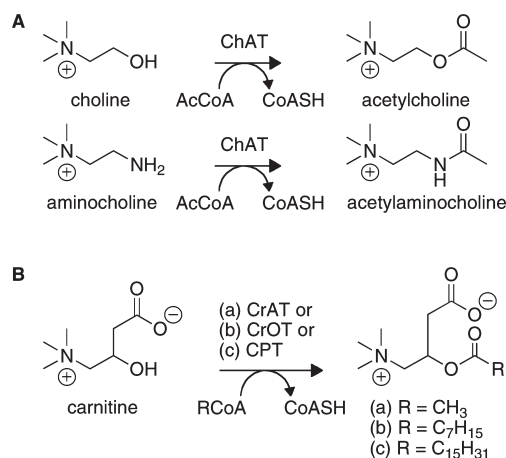


FIGURE 1: Reactions catalyzed by (A) choline acetyltransferase (ChAT) and (B) carnitine acyltransferases (CrAT, CrOT, and CPT).

length (varying from 2 to 16 carbons) of their acyl-chain cosubstrate selectivity (Figure 1B). Carnitine and choline differ only in their substituents at C1, where a carboxymethyl group of carnitine replaces a hydrogen atom in choline. Short-, medium-, and long-chain fatty acids are favored by CrAT, CrOT, and CPTs, respectively. A decrease in CrAT activity has been associated with AD (8), several vascular diseases (9), and ataxic encephalopathy (10).

The crystal structures of rat ChAT (rChAT) (11, 12), human ChAT (hChAT) (13), human CrAT (hCrAT) (14), mouse CrAT (mCrAT) (15), mouse CrOT (mCrOT) (16), two mutants of mCrAT (17), and rat CPTII (rCPTII) (18) have been reported. All these structures are strikingly similar and reveal a common

<sup>†</sup>This work was supported by start-up funds from the Life Sciences Institute and the College of Pharmacy at the University of Michigan (to S.G.-T.). V.R.P. was supported by a Summer Institute Rackham Merit Fellowship (University of Michigan).

\*To whom correspondence should be addressed. E-mail: sylviegt@umich.edu. Phone: (734) 615-2736. Fax: (734) 615-5521.

<sup>1</sup>Abbreviations: CoA, coenzyme A; CrAT, carnitine acetyltransferase; CrOT, carnitine octanoyltransferase; CPT, carnitine palmitoyltransferase; ChAT, choline acetyltransferase; ChOT, choline octanoyltransferase; ChPT, choline palmitoyltransferase; EDTA, ethylenediaminetetraacetic acid; LB, Luria-Bertani broth; SDS-PAGE, sodium dodecyl sulfate-polyacrylamide gel electrophoresis; Tris-HCl, tris(hydroxymethyl)aminomethane hydrochloride.

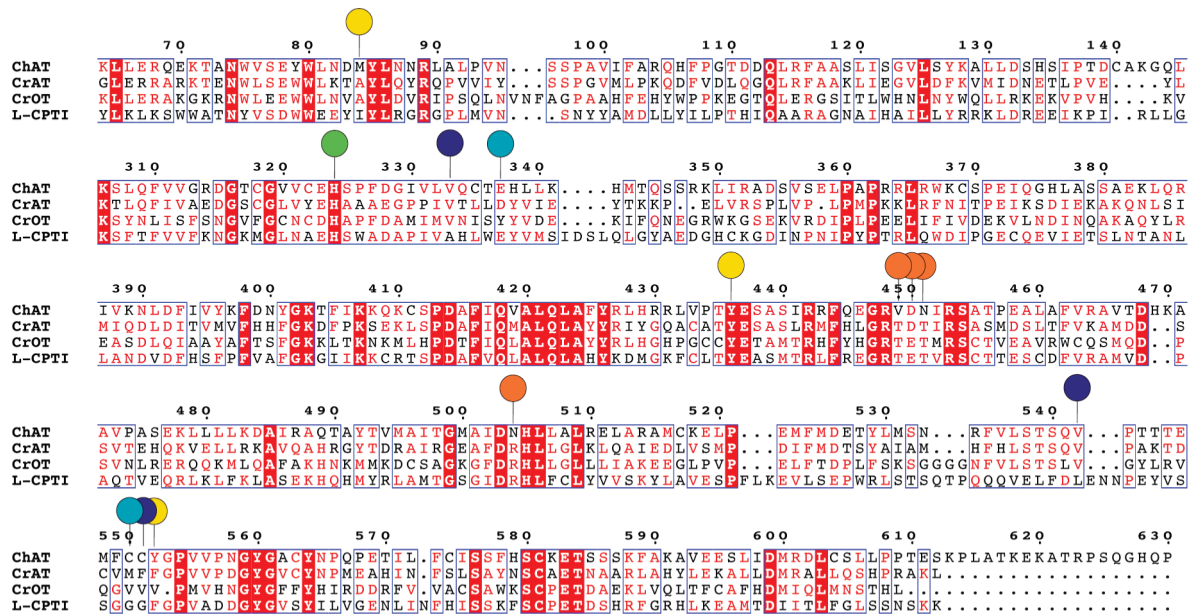


FIGURE 2: Sequence alignment of human ChAT, CrAT, CrOT, and L-CPTI. White letters with a red background denote residues that are fully conserved, whereas red letters denote residues that are highly conserved. Colored circles indicate positions mutated in this study. Yellow circles indicate large residues in the channel on the choline side that we mutated to increase the size of the channel. Turquoise circles indicate mutations made in the CrAT series also made in this study. Dark blue circles indicate residues that we mutated to the residues in CrOT or L-CPTI. The green circle indicates the histidine residue located in the middle of the active site of the enzymes. Orange circles indicate residues mutated by others to convert ChAT into CrAT. The double green line at the right of the top section indicates a gap in the sequences where no mutations were made.

active site located at the interface of the two domains of the enzyme. The active site contains a histidine residue [H324 in hChAT (Figure 2)] required for catalysis positioned in the center of a catalytic tunnel with the choline substrate and CoA cosubstrate lying on opposite sides of the tunnel (19–21). These structures not only provided insights into the mechanism of acyl-chain transfer by these enzymes but also highlighted the important and significant structural differences in their choline/carnitine as well as in their acyl moiety binding regions. A structural model of liver CPTI (L-CPTI) based on the CrAT crystal structure along with kinetic analyses of L-CPTI mutants demonstrated the essential catalytic role of D477 and D567 [corresponding to D328 and D414 of hChAT, respectively (Figure 2)], located near the carnitine and the CoA, respectively (22).

In addition to the structural data, reports on the redesign of CrAT into CrOT (23) and CPT (24) indicated that D356 and M564 residues in rCrAT [corresponding to E337 and C550 in hChAT, respectively (Figure 2)] are critical for dictating the length of the acyl-CoA chains transferred by these enzymes. When compared to the wild-type enzyme, CrAT-M564G and CrAT-M564A mutants displayed higher activity toward medium- to long-chain acyl-CoAs (6–14 carbons) and lower activity toward the natural cosubstrate acetyl-CoA (23). The introduction of an additional mutation site into the CrAT-D356A/M564G double mutant increased the activity toward the long-chain acyl-CoAs (10–18 carbons) (24).

A study of the conversion of rChAT into CrAT showed that mutating ChAT residues V449, D450, N451, and N504 to T, E, T, and R, respectively (Figure 2), accommodated the additional carboxymethyl group of carnitine (25). In addition to the electrostatic and steric factors that govern the ChAT substrate specificity, a close analysis of the hChAT crystal structure (13) in conjunction with our recent report on the substrate and cosubstrate promiscuity of hChAT (26) suggested that mutation of the

M84 residue could potentially increase the size of the tunnel to allow promiscuity for choline substrates with a larger group on their quaternary ammonium center (Figure 3A). A combination of protein alignment data (Figure 2) and structural data (Figure 3A) also suggested that targeting residue Y436 or Y552 could achieve the same purpose. In this study, we interrogate the role that three amino acid residues (M84, Y436, and Y552) play in binding and locking of choline and its analogues into the active site tunnel of hChAT, using single-point mutations.

Herein, we also report the conversion, by site-directed mutagenesis, of hChAT into choline octanoyltransferase (ChOT) and choline palmitoyltransferase (ChPT). In addition to the previously reported E337 and C550 residues (numbering of hChAT) in the CrAT series, we have identified a new amino acid residue (C551) that contributes to the acyl-CoA specificity in hChAT. The hChAT-C551A mutant showed a decrease in activity toward the natural cosubstrate acetyl-CoA but displayed an overall increase in specificity toward all other short-, medium-, and long-chain acyl-CoAs tested. The double hChAT-E337A/C551A mutant exhibited a preference for medium- and long-chain acyl-CoA cosubstrates when compared to the single hChAT-C551A mutant. Interestingly, our work reveals a completely different cosubstrate specificity profile for the hChAT-E337A/C550G, hChAT-C550A, and hChAT-C550G mutants compared to those of their counterparts in the CrAT series. Furthermore, by preparation of a variety of double and triple mutants, we show that the presence of at least one of the cysteine residues (C550 or C551) is required for hChAT specificity toward medium- and long-chain acyl-CoAs. We also demonstrated that mutation of valine 333 to alanine increases the activity of the enzyme with the natural cosubstrate acetyl-CoA.

## MATERIALS AND METHODS

*Bacterial Strains, Plasmids, Materials, and Instrumentation.* The pProEX-HTa plasmid containing the hChAT gene

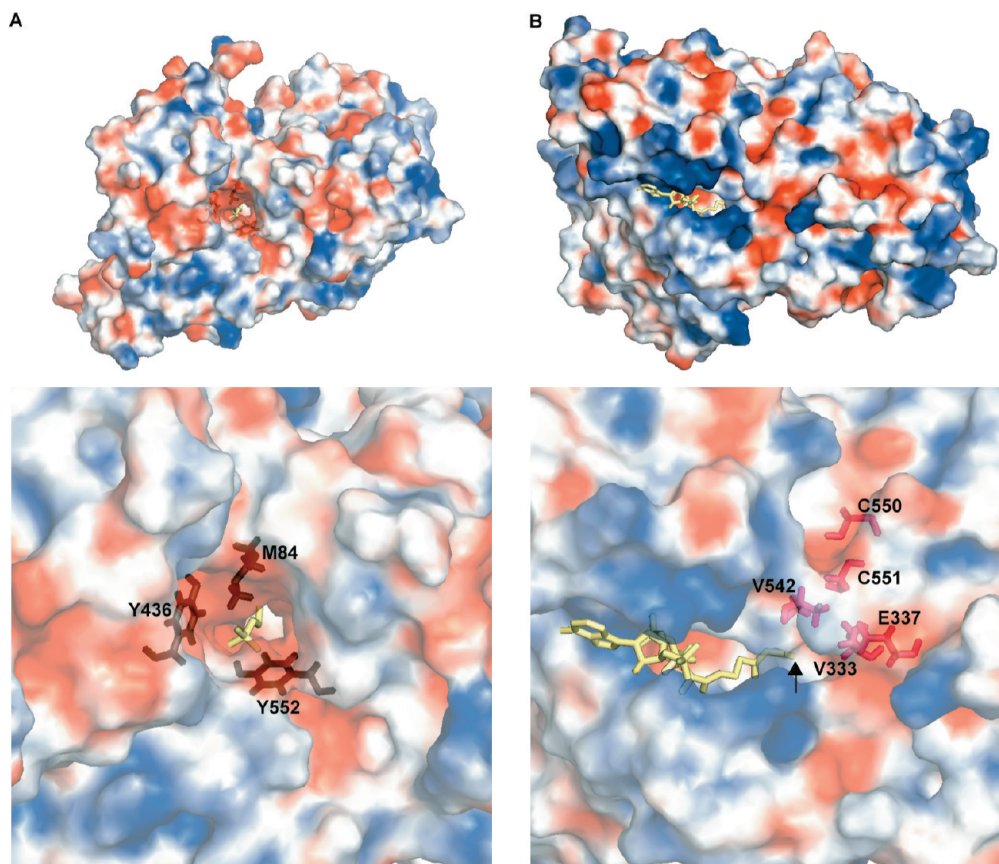


FIGURE 3: Crystal structure of hChAT (Protein Data Bank entries 2FY3 and 2FY4) showing at the top of both panels the tunnels on (A) the choline side and (B) the CoA side. The bottom of both panels focuses on the residues mutated in this study (displayed as sticks and highlighted in dark red on the choline side and in pink on the CoA side). Choline and CoA are colored yellow. The sulfur atom to which the various acyl chains are tethered in thioester linkages to CoA is indicated by a black arrow in panel B. Adaptive Poisson–Boltzmann Solver (APBS) (45) was used as a tool within PyMOL (46) to calculate charges. Settings  $-12$  and  $+12$  were used for negative and positive electrostatic potential, respectively.

was generously provided by B. Shilton (University of Western Ontario, London, ON). Chemically competent *Escherichia coli* TOP10 and BL21(DE3) cell strains were purchased from Invitrogen (Carlsbad, CA). Restriction endonucleases, T4 DNA ligase, and Phusion DNA polymerase were bought from New England BioLabs (NEB, Ipswich, MA). DNA primers for polymerase chain reaction (PCR) were obtained from Integrated DNA Technologies (IDT, Coralville, IA). Int-pET19b-pps containing an N-terminal decahistidine tag separated from the gene by a precision protease cleavage site was generously provided by T. Biswas (University of Michigan) (27). DNA sequencing was performed at the University of Michigan DNA Sequencing Core. All CoA derivatives, aminocholine, choline, and buffer components were purchased from Sigma-Aldrich (Milwaukee, WI) and used without any further purification. We previously reported the synthesis and characterization of all noncommercially available choline derivatives utilized in this study (Figure S1 of the Supporting Information) (26). Fast protein liquid chromatography (FPLC) was performed as the last protein purification step on a Bio-Rad (Hercules, CA) BioLogic DuoFlow system using a HighPrep 26/60 Sephacryl S-200 high-resolution column (GE Healthcare, Piscataway, NJ). Spectrophotometric assays were performed in a high-throughput fashion using a Spectra-Max M5 microplate reader.

**Preparation of hChAT and hChAT Mutant Overexpression Constructs.** The primers used for the amplification of hChAT and mutant hChAT genes are listed in Table S1 of the Supporting Information. PCRs were conducted using Phusion

DNA polymerase as described by NEB. Wild-type (wt) hChAT was constructed in Int-pET19b-pps to serve as a control. Mutants were constructed using the SOE method (28). In the first round of PCR, the sequences downstream and upstream of the mutation(s) were separately amplified using the hChAT-pProEX-HTa plasmid as a template in conjunction with the 5' primer for the mutant with the 3' primer for hChAT and the 5' primer for hChAT with the 3' primer for the mutant, respectively (Table S1). The resulting amplified PCR fragments were gel-purified and subjected to a second round of PCR using the forward and reverse primers for hChAT (Table S1). The newly amplified fragments were then digested with *NdeI* and *XhoI* and subcloned into the linearized Int-pET19b-pps vector via the corresponding *NdeI* and *XhoI* restriction sites to give the single and double mutants M84A, E337A, E337Y, C550G, C550A, C551A, C550G/C551A, C550A/C551A, V333A, V542A, Y436A, and Y552A. To construct the double and triple mutants V333A/E337A, E337A/C550G, E337A/C550A, E337A/C551A, E337A/C550G/C551A, E337A/C550A/C551A, E337Y/C550G, E337Y/C550A, E337Y/C551A, E337Y/C550G/C551A, and E337Y/C550A/C551A, the newly made V333A, E337A, and E337Y mutants were utilized as templates. All expression clones were characterized by DNA sequencing (University of Michigan DNA Sequencing Core).

**Overproduction and Purification of hChAT and hChAT Mutants.** All proteins were expressed in *E. coli* BL21(DE3) grown in LB medium ( $2 \times 1$  L) supplemented with ampicillin ( $100 \mu\text{g}/\text{mL}$ ), flash-frozen, and stored at  $-80^\circ\text{C}$  as previously reported (Figure S2 of the Supporting Information) (26). Protein

Table 1: Kinetic Parameters of hChAT-wt and hChAT-C551A Determined with Aminocholine<sup>a</sup>

enzyme (vector)	CoA derivative	$K_m$ ( $\mu\text{M}$ )	$k_{\text{cat}}$ ( $\text{s}^{-1}$ )	$k_{\text{cat}}/K_m$ ( $\mu\text{M}^{-1} \text{s}^{-1}$ )
hChAT-wt (pProEX-HTa) <sup>b</sup>	acetyl-CoA	$19.4 \pm 1.1^c$	$1.990 \pm 0.012$	0.103
	<i>n</i> -propionyl-CoA	$12.7 \pm 5.2$	$0.197 \pm 0.065$	0.016
hChAT-wt (Int-pET19b-pps)	<i>n</i> -propionyl-CoA	$20.0 \pm 4.7$	$0.613 \pm 0.028$	0.031
hChAT-C551A (Int-pET19b-pps)	acetyl-CoA	$60.8 \pm 6.1$	$7.07 \pm 0.31$	0.116
	<i>n</i> -propionyl-CoA	$13.7 \pm 3.2$	$1.18 \pm 0.06$	0.086
	<i>n</i> -butyryl-CoA	$4.39 \pm 0.47$	$0.226 \pm 0.003$	0.052

<sup>a</sup>Kinetic parameters were determined at pH 7.5. <sup>b</sup>The kinetic parameters for hChAT-wt (pProEX-HTa) were previously reported (26). <sup>c</sup>All errors were established from at least three independent trials of kinetic experiments.

concentrations were determined using a NanoDrop ND-1000 spectrophotometer (Thermo Scientific).

**Characterization of hChAT and Its Mutants.** Spectrophotometric assays for determining the substrate specificity of the hChAT mutants M84A, Y436A, and Y552A monitored at 324 nm the production of 4-thiopyridone from the reaction of 4,4'-dithiodipyridine (DTDP) with the CoA formed by acylation of a variety of choline analogues (Figure S1) (29). The reaction mixtures (200  $\mu\text{L}$ ) containing hChAT (60 nM), DTDP (2 mM), and a choline analogue (2 mM) were in HEPES buffer (50 mM, pH 7.5 adjusted at room temperature). Reactions were initiated with acetyl-CoA (100  $\mu\text{M}$ ) and mixtures incubated at 25 °C for 30 min taking measurements every 30 s in 96-well plates.

Similarly, spectrophotometric assays were performed to determine the cosubstrate specificity of hChAT-wt and the rest of the hChAT mutants. In these cases, the reaction mixtures (100  $\mu\text{L}$ ) contained hChAT (60 nM), DTDP (2 mM), and aminocholine (2 mM) in HEPES buffer (50 mM, pH 7.5 adjusted at room temperature), and reactions were initiated with CoA derivatives (100  $\mu\text{M}$ ).

For the determination of kinetic parameters for the CoA derivatives accepted by hChAT-wt and hChAT mutants, the concentration of the enzymes was 60 nM, the concentration of the aminocholine substrate was kept constant at 5 mM, and the concentration of the CoA derivatives was varied from 0 to 1 mM. All determinations of  $K_m$  and  $k_{\text{cat}}$  were conducted in triplicate. Parameters were calculated using Kaleidograph curve fitting software.

## RESULTS

**Heterologous Expression and Purification of hChAT and Its Mutants.** hChAT-wt and all hChAT mutants were heterologously expressed in *E. coli* as N-terminally His<sub>10</sub>-tagged proteins to establish their substrate and cosubstrate specificity profiles. Enzymes used in activity assays were purified to homogeneity by Ni(II)-NTA affinity chromatography and flash-frozen for storage at -80 °C. Enzymes used in kinetic analysis were subjected to an additional purification step by size exclusion chromatography prior to being stored. As judged by size exclusion chromatography, hChAT and its mutants appear to be purified in monomeric form. Protein yields (in milligrams per liter of culture) were 0.61 (wt), 1.80 (M84A), 0.66 (E337A), 0.89 (E337Y), 1.33 (C550G), 0.18 (C550A), 0.46 (C551A), 1.19 (C550G/C551A), 1.15 (C550A/C551A), 0.66 (E337A/C550G), 0.44 (E337A/C550A), 0.88 (E337A/C551A), 0.06 (E337A/C550G/C551A), 16.2 (E337A/C550A/C551A), 0.66 (E337Y/C550G), 3.38 (E337Y/C550A), 1.19 (E337Y/C551A), 0.49 (E337Y/C550G/C551A), 12.9 (E337Y/C550A/C551A), 1.43 (Y436A), 0.97 (Y552A), 2.31 (V333A), 1.53 (V542A), and 3.78 (V333A/E337A) (Figure S2 of the Supporting Information).

**Kinetic Characterization of hChAT-wt and the hChAT-C551A Mutant.** We previously reported the expression, purification, and characterization of hChAT utilizing an hChAT-pProEX-HTa plasmid (26). In this study, we cloned the hChAT gene into the Int-pET19b-pps vector. Prior to construction of the hChAT mutant clones using the Int-pET19b-pps vector, we determined kinetic parameters for hChAT-wt (Int-pET19b-pps) by UV-vis assays by holding the concentration of hChAT at a final concentration of 60 nM and by varying the concentration of aminocholine and the different cosubstrates and compared them to our previously reported data (Table 1). Aminocholine was used as it was previously found to be a better substrate for hChAT-wt than choline. We found the  $K_m$  value for *n*-propionyl-CoA for hChAT-wt expressed from Int-pET19b-pps ( $20.0 \pm 4.7 \mu\text{M}$ ) to be in good agreement with the  $K_m$  measured using hChAT-wt produced from pProEX-HTa ( $12.7 \pm 5.2 \mu\text{M}$ ). The catalytic turnover ( $k_{\text{cat}}$ ) of  $0.613 \pm 0.028 \text{ s}^{-1}$  and catalytic efficiency ( $k_{\text{cat}}/K_m$ ) of  $0.0310 \mu\text{M}^{-1} \text{ s}^{-1}$  were found to be 3- and 2-fold higher for hChAT-wt expressed from Int-pET19b-pps, respectively. We therefore decided to construct all hChAT mutants using the Int-pET19b-pps vector. As we identified C551 as a novel important residue for dictating the length of the acyl chain accepted by hChAT, we also tested the kinetic parameters of the hChAT-C551A mutant (Table 1). With hChAT-C551A and acetyl-CoA, a  $K_m$  of  $60.8 \pm 6.1 \mu\text{M}$  and a catalytic turnover of  $7.07 \pm 0.31 \text{ s}^{-1}$  resulting in a catalytic efficiency  $0.116 \mu\text{M}^{-1} \text{ s}^{-1}$  were determined. The C551A mutant kinetic parameters were also determined for *n*-propionyl-CoA and *n*-butyryl-CoA. Here,  $K_m$  values of  $13.7 \pm 3.2$  and  $4.39 \pm 0.47 \mu\text{M}$  and catalytic turnover values of  $1.18 \pm 0.06$  and  $0.226 \pm 0.003 \text{ s}^{-1}$  resulted in catalytic efficiencies of 0.086 and  $0.052 \mu\text{M}^{-1} \text{ s}^{-1}$ , respectively.

**Identification of Three Essential Residues for Choline Binding to hChAT.** We have recently demonstrated the ability of hChAT to accept choline derivatives containing a variety of quaternary ammonium centers and a hydroxyl or an amino functionality separated by two methylene groups (26). Cronin showed that ChAT can be converted to CrAT (25), suggesting the ability of ChAT to be mutated to accommodate larger choline derivatives. It is known that in hChAT, the entrance to the substrate tunnel is much wider than that required to accommodate choline and that the tunnel narrows near the choline-binding site, resulting in specificity for choline analogues in which only one of the three methyl groups of the quaternary ammonium center is modified. A close analysis of the hChAT crystal structure showed that residues M84, Y436, and Y552 are found in the narrow part of the substrate tunnel (Figure 3A). With the idea of expanding the promiscuity of hChAT toward choline analogues with larger quaternary ammonium centers, we generated hChAT mutants M84A, Y436A, and Y552A. When tested with

acetyl-CoA, both M84A and Y552A were found to be completely inactive toward choline and all its analogues tested (Figure S3 of the Supporting Information). With acetyl-CoA as a cosubstrate, aminocholine proved to be a weak hChAT-Y436A substrate (24% activity compared to that of hChAT-wt) (data not shown). These results demonstrate the importance of the M84, Y436, and Y552 residues in holding the choline molecule in the hChAT active site.

**Alteration of hChAT Activity and Cosubstrate Specificity by Site-Directed Mutagenesis.** Because of the previous successes in converting CrAT into CrOT and CPT, we predicted that the cosubstrate specificity profile of hChAT could be modified to those of ChOT and ChPT to accommodate medium- and long-chain acyl-CoAs. To confirm this hypothesis, we mutated E337 to alanine to mimic one of the double mutations in the CrAT to CPT alteration (Figure 2) (24). Similarly, the same residue was mutated to tyrosine, because its counterpart in CrOT is a tyrosine. C550 was mutated to glycine and alanine to emulate the previous studies mutating CrAT into CPT and CrOT, respectively (23). As the counterpart amino acid residues in CrOT and CPT are smaller in size than the cysteine at position 551, C551 was mutated to alanine to compensate for the larger size of incoming CoAs. Combinations of all three mutations resulted in the double and triple mutants, which we believed would allow for promiscuity toward larger CoA cosubstrates. V333 and V542 located on the  $\alpha$ -helix adjacent to the CoA binding site (Figure 3B) were also mutated to alanine with the thought that these mutations would allow the longer CoA derivatives to fit adjacent to the helix.

To determine the activity of the hChAT mutants, we tested the enzymes with the substrate aminocholine and several CoA cosubstrates, including acetyl-, *n*-propionyl-, *n*-butyryl-, hexanoyl-, octanoyl-, decanoyl-, lauroyl-, and palmitoyl-CoA. The activities of all hChAT mutants and CoA derivatives were normalized to the rate of the reaction of acetyl-CoA with aminocholine and recombinant wild-type hChAT. Figure 4 and Figure S3 of the Supporting Information show a comparison of the activity of the hChAT mutants with the eight CoAs tested. hChAT mutants E337A, E337Y, C550G/C551A, C550G, E337A/C550G/C551A, E337A/C550A/C551A, E337Y/C550G, E337Y/C550G/C551A, E337Y/C550A/C551A, V542A, and V333A/E337A (Figure S3E–O) showed no or significantly reduced activity with all CoA derivatives. The wild-type hChAT enzyme showed activity with acetyl-CoA (100%) and *n*-propionyl-CoA (28%), whereas all other CoAs had <8% activity (Figure 4A). The E337Y/C551A and C550A/C551A hChAT mutants had 30 and 27% activity with acetyl-CoA, respectively (Figure S3C,D). hChAT-E337Y/C551A displayed low activity with all remaining CoAs, while hChAT-C550A/C551A showed activity with *n*-propionyl-CoA (18%) and *n*-butyryl-CoA (12%) and <5% activity with the remaining CoAs. hChAT-E337A/C550A (Figure S3B) showed activity with acetyl-CoA (12%) and <6% activity with the other CoAs. Interestingly, hChAT-V333A displayed an increase in activity with acetyl-CoA (134%) and activity with *n*-propionyl-CoA (17%), but <5% activity was observed for the remaining CoAs (Figure S3A). hChAT-C551A displayed activity with acetyl-CoA (68%), *n*-propionyl-CoA (59%), *n*-butyryl-CoA (22%), and hexanoyl-CoA (12%), but <4% activity with the longer CoAs (Figure 4B). Mutating hChAT residues E337 and C551 to alanine resulted in activity with acetyl-CoA (27%), *n*-propionyl-CoA (40%), *n*-butyryl-CoA (42%), hexanoyl-CoA (14%), octanoyl-CoA (22%), and decanoyl-CoA (18%), and <5% activity with

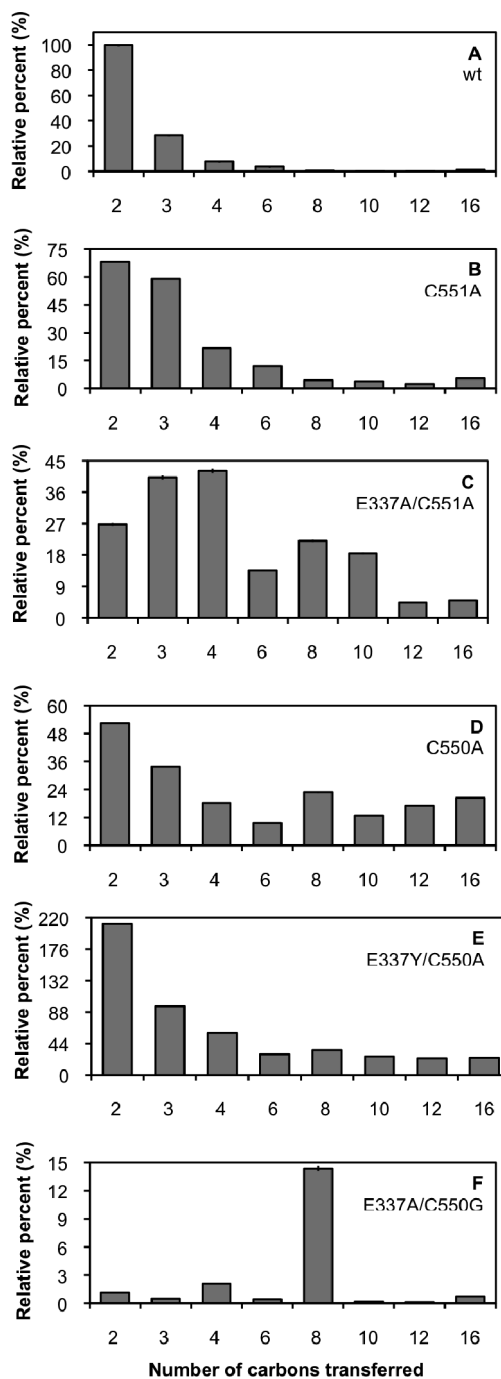


FIGURE 4: Histograms of hChAT mutants comparing the rates of different CoA derivatives, normalized to the rate of the wild-type enzyme with acetyl-CoA, for each mutant: (A) wild-type hChAT, (B) hChAT-C551A, (C) hChAT-E337A/C551A, (D) hChAT-C550A, (E) hChAT-E337Y/C550A, and (F) hChAT-E337A/C550G. The number 2 denotes acetyl-CoA, the number 3 *n*-propionyl-CoA, the number 4 *n*-butyryl-CoA, the number 6 hexanoyl-CoA, the number 8 octanoyl-CoA, the number 10 decanoyl-CoA, the number 12 lauroyl-CoA, and the number 16 palmitoyl-CoA.

lauroyl- and palmitoyl-CoA (Figure 4C). Mutation of C550 to alanine resulted in activity with acetyl-CoA (52%), *n*-propionyl-CoA (34%), *n*-butyryl-CoA (18%), hexanoyl-CoA (10%), octanoyl-CoA (23%), decanoyl-CoA (13%), lauroyl-CoA (17%), and palmitoyl-CoA (20%) (Figure 4D). The mutant with the best overall activity was found to be hChAT-E337Y/C550A, with activity with acetyl-CoA (211%), *n*-propionyl-CoA (96%), *n*-butyryl-CoA (59%), hexanoyl-CoA (29%), octanoyl-CoA

(35%), decanoyl-CoA (26%), and lauroyl- and palmitoyl-CoA (24%) (Figure 4E). Finally, even though it displays low activity (14% with octanoyl-CoA), the mutant hChAT-E337A/C550G was found to be highly specific toward octanoyl-CoA as all other CoAs tested had < 1% activity (Figure 4F).

## DISCUSSION

*Promiscuous Enzymes as Tools for Scaffold Diversification.* Enzymes with diverse biological activities are found to be naturally promiscuous. Many studies on expanding and/or taking advantage of the substrate and cosubstrate promiscuity of enzymes to generate new drugs have been reported (30–34). Garneau-Tsodikova and co-workers took advantage of the natural aminoglycoside substrate and coenzyme A cosubstrate promiscuity of aminoglycoside acetyltransferases to chemoenzymatically generate novel mono-, homodi-, and heterodi-*N*-acylated aminoglycosides (35, 36). Similarly, by using the substrate promiscuity of the arylalkylamine *N*-acetyltransferase (AANAT), Cole and co-workers developed cell-permeable AANAT acetyltransferase inhibitors (37). By revealing the substrate promiscuity of 1-deoxy-D-xylulose 5-phosphate (DXP) synthase, Brammer and Freel Meyers demonstrated the potential of this enzyme as a biocatalyst for the generation of novel  $\alpha$ -hydroxy ketones (38). Glycosyltransferases, key enzymes that catalyze the attachment of a sugar moiety to an aglycone during the biosynthesis of many natural products, also display considerable flexibility toward the sugar donor and/or the acceptor molecule (39–42). However, as exemplified by the glycopeptide glycosyltransferases GtfC and GtfD, not all glycosyltransferases exhibit relaxed substrate specificity (43). By means of directed evolution, Thorson and co-workers expanded the promiscuity of glycosyltransferase enzymes (44).

In this study, we have focused on expanding the coenzyme A cosubstrate promiscuity of the hChAT enzyme by site-directed mutagenesis to generate choline octanoyltransferase (ChOT) and choline palmitoyltransferase (ChPT) enzymes capable of transferring medium and long acyl chains to choline and its analogues, respectively. We have also aimed to generate a ChAT enzyme capable of transferring acyl chains to a variety of choline analogues.

*Conversion of hChAT into ChOT and ChPT.* Substantial efforts dedicated to the conversion of CrAT into CrOT (23) and CPT (24) have identified D356 and M564 [corresponding to E337 and C550 in hChAT (Figure 2)] as important residues for fatty acyl chain length specificity in rCrAT. We hypothesized that similar mutations could lead to the conversion of hChAT into ChOT and ChPT. A close analysis of the hChAT crystal structure suggested that C551, V333, and V542 could also potentially be critical in dictating the length of the acyl chain to be enzymatically transferred to choline and its analogues (Figure 3B). Our investigation began via overexpression of a series of N-terminally His<sub>10</sub>-tagged ChAT mutants in soluble form (Figure S2 of the Supporting Information). To effectively compare the activity of each enzyme, all enzymes were first tested by incubation of aminocholine with the natural cosubstrate acetyl-CoA (Figure 5A). All activities are normalized to the rate of the acetyl-CoA, hChAT-wt, and aminocholine reaction. Aminocholine was used in place of the natural choline substrate as it was previously shown to be a better substrate for hChAT-wt (26). Two mutants were found to give an increase in hChAT activity when reacted with acetyl-CoA and aminocholine. As predicted, the singly mutated hChAT-

V333A enzyme displayed a 1.3-fold increase in activity. Interestingly, the doubly mutated hChAT-E337Y/C550A showed an unexpected 2.1-fold increase in activity. All other mutant enzymes showed a decrease in activity when reacted with aminocholine and acetyl-CoA. In contrast to what we predicted, mutation of valine 542 to alanine (V542A) resulted in a significant decrease in activity with all CoA derivatives tested (Figure 5A and Figure S3N of the Supporting Information). hChAT-E337A exhibited a 4-fold reduction in activity, and E337Y exhibited a 2.5-fold reduction. The C550G mutant exhibited a 10-fold reduction in activity, and when the same residue was mutated to an alanine (C550A), a 2-fold reduction was observed. hChAT-C551A exhibited a 1.5-fold reduction in activity.

Even though the hChAT-E337Y/C550A mutant was found to be the most active when reacted with acetyl-CoA, it was observed that double mutations generally resulted in a larger decrease in activity with acetyl-CoA than single mutations. In fact, an additional mutation to hChAT-V333A, naturally more active than hChAT-wt, led to the hChAT-V333A/E337A mutant displaying a 2.5-fold rate reduction. As expected, changing both glutamate 337 to alanine and cysteine 550 to alanine resulted in a 10-fold reduction in activity, a greater reduction than that observed for the corresponding single mutants hChAT-E337A and hChAT-C550A. Making the E337A/C550G mutations nearly abolished all activity with acetyl-CoA. Mutation of both cysteine residues resulted in 3.5-fold (C550A/C551A) and 7.7-fold (C550G/C551A) decreases in activity. Interestingly, in contrast to hChAT-E337Y/C550A that displays high activity with acetyl-CoA, the hChAT-E337A/C551A, -E337Y/C550G, and -E337Y/C551A mutants exhibited 3.7-, 50-, and 3.5-fold decreases in activity, respectively. All triple mutants resulted in an at least 20-fold reduction in activity. These results not surprisingly indicate that increasing the overall size of the hChAT tunnel on the cosubstrate side generally leads to a decrease in the affinity for the natural acetyl-CoA cosubstrate.

However, as expected, several of the double hChAT mutants, including E337A/C550G, E337A/C551A, and E337Y/C550A, were found to nicely accommodate at least one of the larger CoA derivatives that were tested (Figure 5B,C). Most notable among these mutants is hChAT-E337Y/C550A, for which a 2.1–100-fold increase in activity is observed for the transfer of all short-, medium-, and long-chain acyl-CoAs tested. Not only is hChAT-E337Y/C550A more active with the natural acetyl-CoA cosubstrate than hChAT-wt (2.1-fold increase in activity), it is also the most active enzyme generated against all CoA derivatives tested. Indeed, with hChAT-E337Y/C550A, 3.4-, 7-, 7-, 57-, 130-, 120-, and 24-fold increases in activity are observed during the transfers of the *n*-propionyl, *n*-butyryl, hexanoyl, octanoyl, decanoyl, lauroyl, and palmitoyl chains, respectively. This truly unique mutant exhibiting high cosubstrate flexibility can therefore be characterized as a ChAT, ChOT, and ChPT enzyme. Also worth mentioning is hChAT-E337A/C550G. This double mutant originally designed to mimic its previously reported counterpart in the carnitine series, CrAT-D356A/M564G, displaying activity toward a variety of medium- and long-chain acyl-CoAs (6–18 carbons) (24), was unexpectedly found to be a truly inflexible ChOT (Figure 5B,C). Indeed, hChAT-E337A/C550G shows minute activity with all CoA derivatives tested with the exception of octanoyl-CoA, where a 23-fold increase in activity is observed when compared to that of hChAT-wt subjected to the same reaction conditions. The discrepancy in the cosubstrate specificity profile between the carnitine and choline series also holds

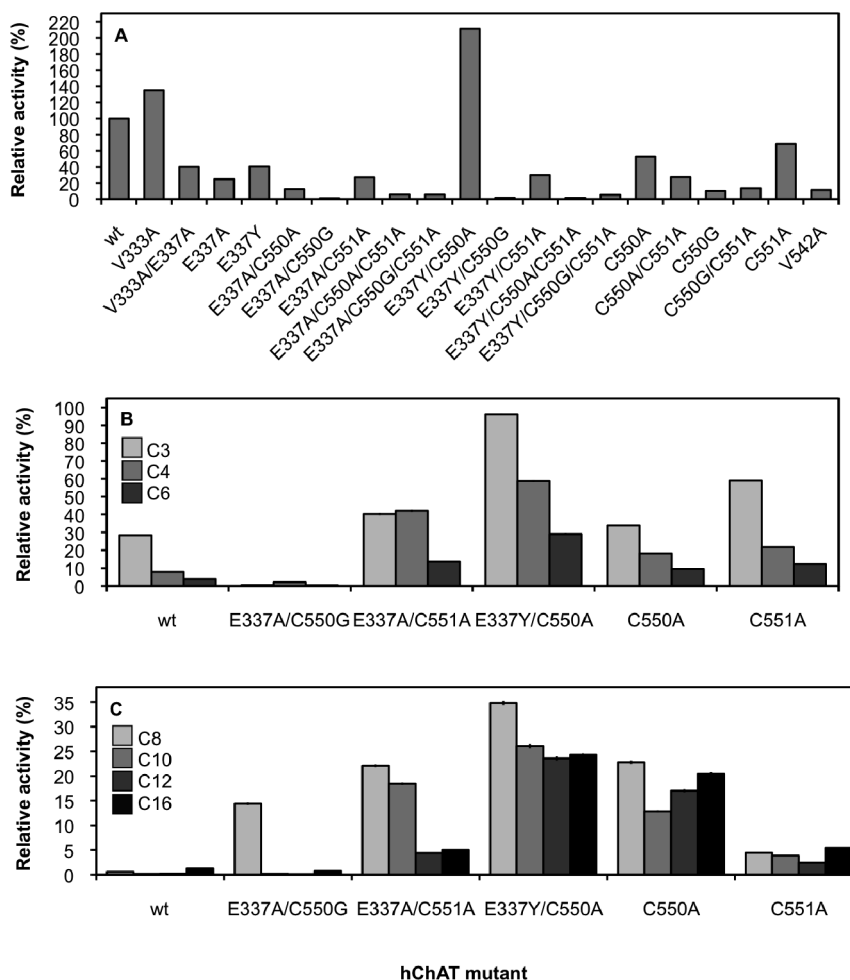


FIGURE 5: Histograms comparing the normalized rates of (A) acetyl-CoA with all hChAT mutants, (B) *n*-propionyl-CoA, *n*-butyryl-CoA, and hexanoyl-CoA, and (C) octanoyl-CoA, decanoyl-CoA, lauroyl-CoA, and palmitoyl-CoA with selected mutants. All rates are normalized to the rate of hChAT-wt with acetyl-CoA.

true for the single mutants hChAT-C550G and -C550A prepared as mimics of the CrAT-M564G and M564A enzymes, respectively (23). In contrast to the M564G mutation in CrAT that results in an increase in activity with medium- and long-chain acyl-CoAs (4–16 carbons), the corresponding C550G mutation in hChAT does not lead to its conversion to either ChOT or ChPT (Figure S3G of the Supporting Information). However, mutation of this amino acid residue to alanine (C550A) results in conversion of the enzyme to ChPT with some observable ChOT activity. Interestingly, in the carnitine series, even though it displays cosubstrate promiscuity toward medium- and long-chain acyl-CoAs, CrAT-M564A is found to be less active than CrAT-M564G.

In this study, in addition to E337 and C550, we have identified C551 as a key residue involved in dictating hChAT cosubstrate specificity. The C551A single mutation results in an overall increase in ChOT and ChPT activity. More specifically, 2-, 3-, 3-, 7-, 20-, 10-, and 5-fold increases in activity are observed during the transfers of the *n*-propionyl, *n*-butyryl, hexanoyl, octanoyl, decanoyl, lauroyl, and palmitoyl chains, respectively, by hChAT-C551A (Figure 5B,C). Kinetic characterization of this mutant also reveals its increased catalytic efficiency with respect to transferring the *n*-propionyl and *n*-butyryl chain to aminocholine (Table 1). The hChAT-E337A/C551A double mutant actually displays better ChOT and ChPT activity than hChAT-C551A.

Not shown in Figure 5, but worthy of mention, are hChAT-E337A/C550A and hChAT-E337Y/C551A (Figure S3B,D of the Supporting Information). hChAT-E337Y/C551A shows reduced activity with the shorter CoA derivatives (acetyl-CoA, *n*-propionyl-CoA, and *n*-butyryl-CoA) but has an approximately 4-fold increase in activity with the longer CoA derivatives (Figure S3D). Enzymatic reactions with hChAT-E337A/C550A result in decreased rates with all CoAs except palmitoyl-CoAs, where a 5-fold increase is observed (Figure S3B). The low ChOT and ChPT activity of the hChAT-E337A/C550A and -E337Y/C551A mutants is somewhat surprising and indicates that the effects resulting from each mutation are not additive. Interestingly, the C550A/C551A mutation gives no significant increase in rate with either *n*-propionyl-CoA or *n*-butyryl-CoA, corroborating the nonadditivity of the mutations (Figure S3C). Simply put, the additive effects of single and double mutants cannot easily be predicted. Further structural studies will be required to fully understand the rules governing the hChAT cosubstrate selectivity.

*Importance of M84, Y436, and Y552 for Choline Binding to hChAT.* Having generated hChAT mutants able to catalyze the transfer of a variety of acyl chains to aminocholine, we sought to expand the substrate promiscuity of this enzyme. A close look at the hChAT structure reveals a large tunnel entrance that narrows near the choline-binding site. M84, Y436, and Y552 are located in the narrow part of the hChAT substrate tunnel near

the choline quaternary ammonium center (Figure 3A). We hypothesized that mutation of these residues to alanine could widen the narrow part of the tunnel and potentially allow the enzyme to utilize choline analogues with larger quaternary ammonium centers for the production of novel acetylcholine analogues. Unfortunately, mutations at these positions mostly abolish activity toward choline and all choline analogues tested (Figure S1 of the Supporting Information). The characterization of these constructs provides experimental support to validate the role of these three amino acid residues in binding and keeping the choline substrate in the hChAT active site tunnel.

In summary, we have presented evidence that, as in the carnitine series (conversion of CrAT to CrOT and CPT), the cosubstrate promiscuity of hChAT can be expanded from short- to medium-chain (ChOT) and long-chain (ChPT) acyl-CoAs. In addition to the previously mentioned E337 and C550 residues, we have identified a novel amino acid residue, C551, critical to dictating chain length specificity in hChAT. We have demonstrated that the presence of at least one of two cysteine residues, C550 or C551, is necessary for chain length specificity in hChAT. We have also identified M84, Y436, and Y552 as critical amino acid residues for binding and locking of choline and its analogues into the active site tunnel of the hChAT enzyme. In conjunction with our previously reported characterization of the substrate promiscuity of hChAT-wt (26), this work sets the stage for the production of libraries of novel acetylcholine analogues as potential cholinesterase inhibitors.

#### ACKNOWLEDGMENT

Prof. Brian H. Shilton (University of Western Ontario) is acknowledged for the generous gift of the hChAT-containing plasmid. We thank Dr. Tapan Biswas (University of Michigan) for help in generating Figure 3 as well as for the gift of the Int-pET19b-pps vector. We thank Dr. Mi Hee Lim for the use of equipment.

#### SUPPORTING INFORMATION AVAILABLE

A table of primers used in this study (Table S1), structures of substrates and cosubstrates tested with the hChAT-M84A, -Y436A, and -Y552A mutants (Figure S1), gel containing Ni(II)-NTA-purified proteins (Figure S2), histograms of hChAT mutants comparing the rates of different CoA derivatives (Figure S3), and representative examples of kinetic curves (Figure S4). This material is available free of charge via the Internet at <http://pubs.acs.org>.

#### REFERENCES

- Whitehouse, P. J. (1998) The cholinergic deficit in Alzheimer's disease. *J. Clin. Psychiatry* 59 (Suppl. 13), 19–22.
- Oda, Y. (1999) Choline acetyltransferase: The structure, distribution and pathologic changes in the central nervous system. *Pathol. Int.* 49, 921–937.
- Holt, D. J., Bachus, S. E., Hyde, T. M., Wittie, M., Herman, M. M., Vangel, M., Saper, C. B., and Kleinman, J. E. (2005) Reduced density of cholinergic interneurons in the ventral striatum in schizophrenia: An in situ hybridization study. *Biol. Psychiatry* 58, 408–416.
- Massouh, M., Wallman, M. J., Pourcher, E., and Parent, A. (2008) The fate of the large striatal interneurons expressing calretinin in Huntington's disease. *Neurosci. Res.* 62, 216–224.
- Mallard, C., Tolcos, M., Leditschke, J., Campbell, P., and Rees, S. (1999) Reduction in choline acetyltransferase immunoreactivity but not muscarinic-m2 receptor immunoreactivity in the brainstem of SIDS infants. *J. Neuropathol. Exp. Neurol.* 58, 255–264.
- Jellinger, K. A. (2003) Rett Syndrome: An update. *J. Neural Transm.* 110, 681–701.
- Jogl, G., Hsiao, Y. S., and Tong, L. (2004) Structure and function of carnitine acyltransferases. *Ann. N.Y. Acad. Sci.* 1033, 17–29.
- Makar, T. K., Cooper, A. J., Tofel-Greth, B., Thaler, H. T., and Blass, J. P. (1995) Carnitine, carnitine acetyltransferase, and glutathione in Alzheimer brain. *Neurochem. Res.* 20, 705–711.
- Melegh, B., Seress, L., Bedekovics, T., Kispal, G., Sumegi, B., Trombitas, K., and Mehes, K. (1999) Muscle carnitine acetyltransferase and carnitine deficiency in a case of mitochondrial encephalomyopathy. *J. Inherited Metab. Dis.* 22, 827–838.
- DiDonato, S., Rimoldi, M., Moise, A., Bertagnoglio, B., and Uziel, G. (1979) Fatal ataxic encephalopathy and carnitine acetyltransferase deficiency: A functional defect of pyruvate oxidation? *Neurology* 29, 1578–1583.
- Cai, Y., Cronin, C. N., Engel, A. G., Ohno, K., Hersh, L. B., and Rodgers, D. W. (2004) Choline acetyltransferase structure reveals distribution of mutations that cause motor disorders. *EMBO J.* 23, 2047–2058.
- Govindasamy, L., Pedersen, B., Lian, W., Kukar, T., Gu, Y., Jin, S., Agbandje-McKenna, M., Wu, D., and McKenna, R. (2004) Structural and functional implications of choline acetyltransferase. *J. Struct. Biol.* 148, 226–235.
- Kim, A. R., Rylett, R. J., and Shilton, B. H. (2006) Substrate binding and catalytic mechanism of human choline acetyltransferase. *Biochemistry* 45, 14621–14631.
- Wu, D., Govindasamy, L., Lian, W., Gu, Y., Kukar, T., Agbandje-McKenna, M., and McKenna, R. (2003) Structure of human carnitine acetyltransferase. Molecular basis for fatty acyl transfer. *J. Biol. Chem.* 278, 13159–13165.
- Jogl, G., and Tong, L. (2003) Crystal structure of carnitine acetyltransferase and implications for the catalytic mechanism and fatty acid transport. *Cell* 112, 113–122.
- Jogl, G., Hsiao, Y. S., and Tong, L. (2005) Crystal structure of mouse carnitine octanoyltransferase and molecular determinants of substrate selectivity. *J. Biol. Chem.* 280, 738–744.
- Hsiao, Y. S., Jogl, G., and Tong, L. (2004) Structural and biochemical studies of the substrate selectivity of carnitine acetyltransferase. *J. Biol. Chem.* 279, 31584–31589.
- Hsiao, Y. S., Jogl, G., Esser, V., and Tong, L. (2006) Crystal structure of rat carnitine palmitoyltransferase II (CPT-II). *Biochem. Biophys. Res. Commun.* 346, 974–980.
- Brown, N. F., Anderson, R. C., Caplan, S. L., Foster, D. W., and McGarry, J. D. (1994) Catalytically important domains of rat carnitine palmitoyltransferase II as determined by site-directed mutagenesis and chemical modification. Evidence for a critical histidine residue. *J. Biol. Chem.* 269, 19157–19162.
- Morillas, M., Clotet, J., Rubi, B., Serra, D., Asins, G., Arino, J., and Hegardt, F. G. (2000) Identification of the two histidine residues responsible for the inhibition by malonyl-CoA in peroxisomal carnitine octanoyltransferase from rat liver. *FEBS Lett.* 466, 183–186.
- Morillas, M., Gomez-Puertas, P., Roca, R., Serra, D., Asins, G., Valencia, A., and Hegardt, F. G. (2001) Structural model of the catalytic core of carnitine palmitoyltransferase I and carnitine octanoyltransferase (COT): Mutation of CPT I histidine 473 and alanine 381 and COT alanine 238 impairs the catalytic activity. *J. Biol. Chem.* 276, 45001–45008.
- Morillas, M., Lopez-Vinas, E., Valencia, A., Serra, D., Gomez-Puertas, P., Hegardt, F. G., and Asins, G. (2004) Structural model of carnitine palmitoyltransferase I based on the carnitine acetyltransferase crystal. *Biochem. J.* 379, 777–784.
- Cordente, A. G., Lopez-Vinas, E., Vazquez, M. I., Swiegers, J. H., Pretorius, I. S., Gomez-Puertas, P., Hegardt, F. G., Asins, G., and Serra, D. (2004) Redesign of carnitine acetyltransferase specificity by protein engineering. *J. Biol. Chem.* 279, 33899–33908.
- Cordente, A. G., Lopez-Vinas, E., Vazquez, M. I., Gomez-Puertas, P., Asins, G., Serra, D., and Hegardt, F. G. (2006) Mutagenesis of specific amino acids converts carnitine acetyltransferase into carnitine palmitoyltransferase. *Biochemistry* 45, 6133–6141.
- Cronin, C. N. (1998) Redesign of choline acetyltransferase specificity by protein engineering. *J. Biol. Chem.* 273, 24465–24469.
- Green, K. D., Fridman, M., and Garneau-Tsodikova, S. (2009) hChAT: A tool for the chemoenzymatic generation of potential acetyl/butyrylcholinesterase inhibitors. *ChemBioChem* 10, 2191–2194.
- Biswas, T., and Tsodikov, O. V. (2008) Hexameric ring structure of the N-terminal domain of *Mycobacterium tuberculosis* DnaB helicase. *FEBS J.* 275, 3064–3071.
- Ho, S. N., Hunt, H. D., Horton, R. M., Pullen, J. K., and Pease, L. R. (1989) Site-directed mutagenesis by overlap extension using the polymerase chain reaction. *Gene* 77, 51–59.

29. Magalhaes, M. L., and Blanchard, J. S. (2005) The kinetic mechanism of AAC3-IV aminoglycoside acetyltransferase from *Escherichia coli*. *Biochemistry* 44, 16275–16283.
30. Fridman, M., Balibar, C. J., Lupoli, T., Kahne, D., Walsh, C. T., and Garneau-Tsodikova, S. (2007) Chemoenzymatic formation of novel aminocoumarin antibiotics by the enzymes CouN1 and CouN7. *Biochemistry* 46, 8462–8471.
31. Freil Meyers, C. L., Oberthur, M., Heide, L., Kahne, D., and Walsh, C. T. (2004) Assembly of dimeric variants of coumermycins by tandem action of the four biosynthetic enzymes CouL, CouM, CouP, and NovN. *Biochemistry* 43, 15022–15036.
32. Steffan, N., and Li, S. M. (2009) Increasing structure diversity of prenylated diketopiperazine derivatives by using a 4-dimethylallyl-tryptophan synthase. *Arch. Microbiol.* 191, 461–466.
33. Liu, X., and Walsh, C. T. (2009) Characterization of cyclo-acetoacetyl-L-tryptophan dimethylallyltransferase in cyclopiazonic acid biosynthesis: Substrate promiscuity and site directed mutagenesis studies. *Biochemistry* 48, 11032–11044.
34. Monsan, P., Remaud-Simeon, M., and Andre, I. (2010) Transglucosidases as efficient tools for oligosaccharide and glucoconjugate synthesis. *Curr. Opin. Microbiol.* 13, 293–300.
35. Green, K. D., Chen, W., Houghton, J. L., Fridman, M., and Garneau-Tsodikova, S. (2010) Exploring the substrate promiscuity of drug-modifying enzymes for the chemoenzymatic generation of N-acylated aminoglycosides. *ChemBioChem* 11, 119–126.
36. Houghton, J. L., Green, K. D., Chen, W., and Garneau-Tsodikova, S. (2010) The future of aminoglycosides: The end or renaissance? *ChemBioChem* 11, 880–902.
37. Zheng, W., Scheibner, K. A., Ho, A. K., and Cole, P. A. (2001) Mechanistic studies on the alkyltransferase activity of serotonin N-acetyltransferase. *Chem. Biol.* 8, 379–389.
38. Brammer, L. A., and Meyers, C. F. (2009) Revealing substrate promiscuity of 1-deoxy-D-xylulose 5-phosphate synthase. *Org. Lett.* 11, 4748–4751.
39. Harle, J., and Bechthold, A. (2009) Chapter 12. The power of glycosyltransferases to generate bioactive natural compounds. *Methods Enzymol.* 458, 309–333.
40. Williams, G. J., Goff, R. D., Zhang, C., and Thorson, J. S. (2008) Optimizing glycosyltransferase specificity via “hot spot” saturation mutagenesis presents a catalyst for novobiocin glycorandomization. *Chem. Biol.* 15, 393–401.
41. Zhang, C., Albermann, C., Fu, X., Peters, N. R., Chisholm, J. D., Zhang, G., Gilbert, E. J., Wang, P. G., Van Vranken, D. L., and Thorson, J. S. (2006) RebG- and RebM-catalyzed indolocarbazole diversification. *ChemBioChem* 7, 795–804.
42. Faridmoayer, A., Fentabil, M. A., Haurat, M. F., Yi, W., Woodward, R., Wang, P. G., and Feldman, M. F. (2008) Extreme substrate promiscuity of the *Neisseria* oligosaccharyl transferase involved in protein O-glycosylation. *J. Biol. Chem.* 283, 34596–34604.
43. Oberthur, M., Leimkuhler, C., Kruger, R. G., Lu, W., Walsh, C. T., and Kahne, D. (2005) A systematic investigation of the synthetic utility of glycopeptide glycosyltransferases. *J. Am. Chem. Soc.* 127, 10747–10752.
44. Williams, G. J., Zhang, C., and Thorson, J. S. (2007) Expanding the promiscuity of a natural-product glycosyltransferase by directed evolution. *Nat. Chem. Biol.* 3, 657–662.
45. Baker, N. A., Sept, D., Joseph, S., Holst, M. J., and McCammon, J. A. (2001) Electrostatics of nanosystems: Application to microtubules and the ribosome. *Proc. Natl. Acad. Sci. U.S.A.* 98, 10037–10041.
46. DeLano, W. L. (2008) The PyMOL Molecular Graphics System, DeLano Scientific LLC, San Carlos, CA.